

Low magnetic field cooling of lepton plasmas via cyclotron-cavity resonance

E. D. Hunter,¹ N. Evetts,² J. Fajans,^{1,a)} W. N. Hardy,² H. Landsberger,¹ R. Mcpeters,¹ and J. S. Wurtele¹

¹Department of Physics, University of California, Berkeley, California 94720, USA

²Department of Physics and Astronomy, University of British Columbia, Vancouver, British Columbia V6T 1Z4, Canada

(Received 27 September 2017; accepted 27 November 2017; published online 12 December 2017)

Pure electron or pure positron plasmas held in magnetic fields B radiate energy because of the cyclotron motion of the plasma particles; nominally, the plasmas should cool to the often cryogenic temperatures of the trap in which they are confined. However, the cyclotron cooling rate for leptons is $(1/4\text{ s})(B/1\text{ T})^2$, and significant cooling is not normally observed unless $B \geq 1\text{ T}$. Cooling to the trap temperatures of $\sim 10\text{ K}$ is particularly difficult to attain. Here, we show that dramatically higher cooling rates ($\times 100$) and lower temperatures ($\div 1000$) can be obtained if the plasmas are held in electromagnetic cavities rather than in effectively free space conditions. We find that plasmas with up to 10^7 particles can be cooled in fields close to 0.15 T , much lower than 1 T commonly thought to be necessary to obtain plasma cooling. Appropriate cavities can be constructed with only minor modifications to the standard Penning-Malmberg trap structures.

Published by AIP Publishing. <https://doi.org/10.1063/1.5006700>

I. INTRODUCTION

Nonneutral plasmas consist of particles of only a single sign of charge. Such plasmas have been studied extensively since the mid-1970s,^{1–3} and may be made from many different constituents. Here, we concentrate on nonneutral plasmas commonly cooled by cyclotron cooling: electron and positron plasmas.

It is often beneficial to obtain very low temperature plasmas. For instance, the number of antihydrogen atoms trapped by the CERN's ALPHA experiment is a strong inverse function of the temperature of the positrons from which the antiatoms are synthesized. Similarly, monoenergetic positron beams are best obtained from very low temperature positron plasmas.⁴

Nonneutral plasmas are typically confined in Penning-Malmberg traps,¹ which employ axial magnetic fields B for radial plasma confinement. These magnetic fields cause the plasma particles to follow gyro orbits, and lose energy by cyclotron radiation. The temperature T of these plasmas can be most simply modeled by $dT/dt = -\Gamma(T - T_B) + H$, where the cooling rate Γ often approaches the free-space cooling rate $\Gamma_0 = (1/4\text{ s})(B/1\text{ T})^2$, T_B is the temperature of the local radiation environment surrounding the plasmas, typically near the temperature of the trap walls, and H represents the heating power coupled into the plasma. The equilibrium or final temperature T_F of the plasmas is trivially found to be

$$T_F = T_B + H/\Gamma \quad (1)$$

and is often observed to be hundreds, even thousands of kelvin, despite $T_B < 10\text{ K}$, unless great care is taken to minimize H . Even with such care, the equilibrium temperatures are rarely lower than 30 K .

Previously,⁵ we showed that resonant cooling using electromagnetic cavities can significantly enhance the plasma cooling rate and lower the equilibrium temperature. This work was inspired by Purcell,⁶ and predicted to occur in plasmas by O'Neil.⁷ Our prior work, however, did not yield plasma temperatures approaching the wall temperatures for plasmas containing more than $\sim 10^5$ particles. (Other prior work was on single electrons,⁸ or on nonequilibrium parametrically-driven electron clouds.⁹ Neither of these last two experiments made direct temperature measurements.) Here, we describe the cooling of many millions of electrons to near-thermal equilibrium with the trap walls in remarkably low magnetic fields, fields low enough to be obtained with copper rather than superconducting magnets.

II. EXPERIMENTAL CYCLE

The plasma diagnostics we use for the experiments described here are destructive. Consequently, we operate with repeated, near-identical inject–hold–dump cycles, similar to those used in many Penning-Malmberg trap experiments.¹ As shown in Fig. 1(a), plasmas are produced by an electron gun, and, following a strong axial magnetic field, passed through a 1 cm ID copper iris where they are then loaded into a microwave cavity. The plasmas are allowed to cool via cyclotron radiation in the cavity, and dumped, through another iris, onto a high-gain charge collector¹⁰ to recover the plasma temperature.¹¹ The irises prevent thermal microwaves (with frequencies below the cut-off frequency of the iris structure) from entering the trap and causing unwanted heating of the plasmas.

We measure plasma temperature by slowly reducing the confining potential on the downstream electrodes and monitoring the amount of charge released. This gives us information about the high-energy tail of the axial velocity distribution,¹¹ in particular, the exponential slope of this

^{a)}joel@physics.berkeley.edu

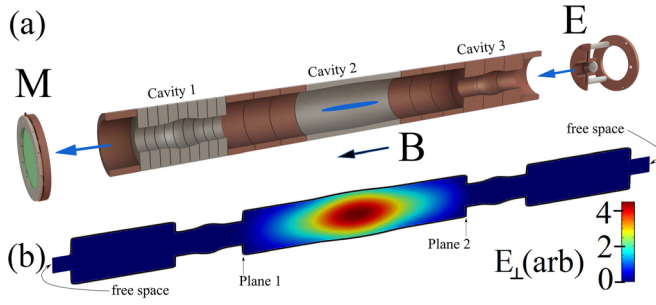


FIG. 1. (a) Sectioned schematic of the Penning-Malmberg trap used in these experiments. Radial confinement is provided by an axial magnetic field B , and axial confinement is provided by potentials applied to the trap electrodes. Electrons are injected into the trap from an electron gun (E) and plasmas are stored in Cavity 2. The plasma temperature and the number of plasma particles are determined by releasing the plasma onto the microchannel plate (MCP)–phosphor screen detector (M). Irises (not shown) are present on both ends of the system. (b) The simulated electric field intensity for the TE_{111} cavity mode.

curve gives the axial plasma temperature T_{\parallel} . At the low magnetic fields considered in this paper, our plasmas are always in the weakly magnetized regime and so T_{\parallel} is expected to thermalize with the cyclotron-cooled component T_{\perp} at the modified Ichimaru-Rosenbluth collision rate.¹² We calculate a collision rate $\nu \approx 100 \text{ s}^{-1}$ for the hottest, least dense plasmas considered here (10^4 K , 10^7 cm^{-3}); for more typical plasmas (100 K , 10^8 cm^{-3}), the theoretical collision rate is $\nu \approx 10^6 \text{ s}^{-1}$.

III. CAVITY

In this paper, we focus on Cavity 2 in Fig. 1(a); the other cavities were not used. This cavity differs from our previous “bulge” cavity (Cavity 3)¹³ as described below:

1. The central bulge in the cavity is very small ($\Delta r = 0.5 \text{ mm}$) relative to the cavity’s radius near its ends (20 mm). The cavity also extends over a much greater length ($L = 9 \text{ cm}$) than our prior cavity.
2. The cavity is made of a single solid electrode. Our previous cavity was made from multiple electrodes and required inter-electrode chokes to limit radiation leakage.
3. The cavity is made from titanium TiAl6V4 alloy, which retains a roughly constant bulk resistivity $\rho \approx 1.6 \mu\Omega \cdot \text{m}$ down to the electrode operating temperature of 9.1 K. In our previous work, the cavity was made with nichrome-coated copper. In order to remove energy from the cavity mode rapidly enough to cool large numbers of electrons, it is essential that the cavity walls remain appropriately resistive at low temperatures. The titanium alloy is believed to be superior to the nichrome used previously because it is only weakly paramagnetic and does not require electroplating, which may not yield a layer several skin-depths thick at the mode frequency.

Although the bulge in the Cavity 2 electrode is able to completely contain certain high-frequency, high-order, microwave modes, the mode confinement from the bulge alone is relatively poor for the low-frequency, low-order, TE_{11k} modes discussed in this paper. (Here, k is the index for the z -dependence of the mode.) Fortunately, the radial steps at Planes 1

and 2 at the entrances to Cavities 1 and 3 (see Fig. 1) improve the TE_{11k} confinement. For example, the TE_{111} mode has a calculated resonant frequency $f \approx 4.397 \text{ GHz}$, and a calculated quality factor $Q = 1000$ set by roughly equal ohmic losses in the resistive cavity wall and radiative losses through the axial opening and inter-electrode gaps ($< 1 \text{ mm}$). Figure 1(b) shows the magnitude of the perpendicular electric field of this mode.

IV. COOLING RATE MEASUREMENTS

A. Dependence on the mode

To test the mode predictions, we scanned the magnetic field through the range of fields predicted by our simulations to include the TE_{11k} modes. (The magnetic field values can be related to radial cyclotron frequencies via the relation $\omega_c = eB/m$, where e is the electron charge and m is the electron mass.) For every B value, we held a plasma with $N = 2 \times 10^6$ electrons, initially at 26 000 K, for 8 s. The resulting final temperatures are plotted in Fig. 2 as a function of B . The measured cooling peak fields and frequencies agree with the mode frequency simulations to about one percent for the modes shown. The dominant cooling peak occurs at $B = 0.1555 \text{ T}$, which, with a cyclotron frequency of 4.353 GHz, is very close to the calculated frequency of the TE_{111} cavity mode. We focus on this mode henceforth.

B. Dependence on the magnetic field

In Fig. 3(a), we show the effect of varying the magnetic field for plasmas containing 2×10^6 electrons; each plasma is cooled for 12 s after being loaded into the cavity. The plasma temperature falls by over two orders of magnitude in the vicinity of the TE_{111} mode. By obtaining similar curves for variable holding times, we can generate a plot of temperature vs. time for each magnetic field value, and from these plots extract the cooling rate Γ as a function of the magnetic field. This is shown in Fig. 3(b), with a representative temperature vs. time curve shown in Fig. 3(c).

The peak measured value of the cooling rate is $\Gamma \approx 0.7 \text{ s}^{-1}$, while the calculated free space cooling rate at 0.1555 T is $\Gamma_0 \approx 0.006 \text{ s}^{-1}$. Hence, the enhancement of Γ over its free space value is greater than 100.

The lowest off-resonance Γ , found in the wings of the curve in Fig. 3(b) [and also in the off-resonance data in

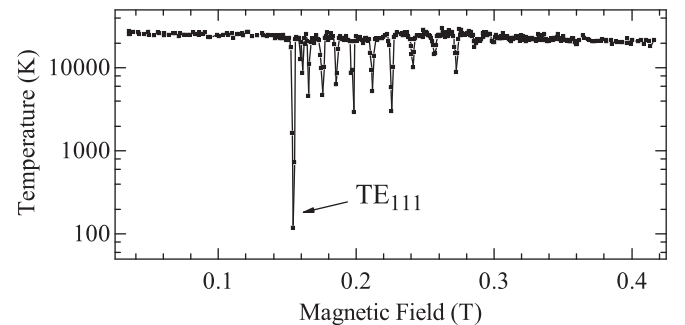


FIG. 2. Measured temperatures of plasmas initialized at 26 000 K and cooled for 8 s at the indicated magnetic field values. The dips occur when the TE_{11k} modes are excited.

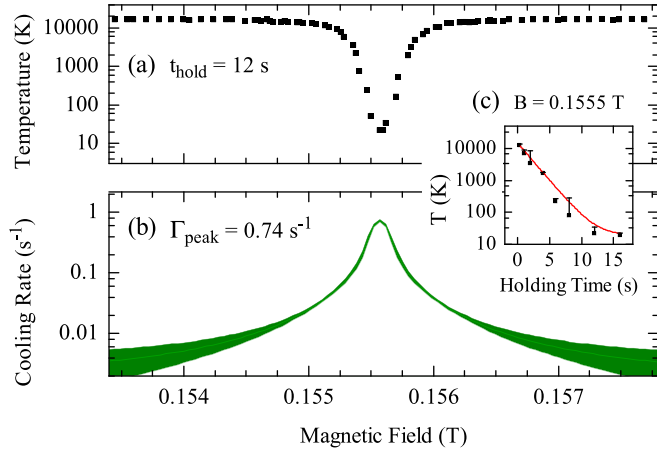


FIG. 3. (a) Plasma temperature after 12 s and (b) cooling rate for 2×10^6 electrons, both measured as the magnetic field is swept. The band indicates the 1σ range around the best fit values. The inset (c) shows typical cooling data at one magnetic field value and the fit from which the cooling rate is derived.

Fig. 4(a)], appears to be lower than the calculated free space rate. This could be evidence of suppressed free-space emission; because of the irises at the extreme ends of the system, there is no easy path for ~ 4 GHz radiation to propagate out of the system.

C. Dependence on the number of electrons N

In order to study the N dependence, we held the magnetic field at the on-resonance value $B = 0.1555$ T, corresponding to the TE_{111} mode, and took temperature vs. time curves for plasmas with N varying from 10^3 to 10^8 electrons. We plot the resulting cooling rate Γ as a function of N in Fig. 4(a), along with measurements of the background rate taken at the off-resonance values $B = 0.153$ and $B = 0.158$ T. In Fig. 4(b), we show the final temperature reached in each case, either after 100 s of cooling, or after attaining equilibrium, which may occur much faster for the on-resonance data points.

For larger numbers of electrons, the frequency of the cyclotron mode will be shifted down slightly via a self-field effect.² Self-field cyclotron mode shifts have been revisited recently in ion-based plasmas¹⁴ and can be understood in our parameter regime as a doppler shift due to the increased $E \times B$ rotation rate for denser plasmas. The on-resonance data in Fig. 4 was taken at fixed B ; we did not continually adjust B to match the peak as N changes, and therefore, some of the reduction in the cooling rate at high N could be due to the cyclotron mode shifting slightly out of resonance with the cavity mode. We estimate the relative magnitude of the frequency shift to be $\sim 10^{-4}$ for our densest plasmas (10^9 cm^{-3}). Assuming the cooling peak has approximately the same shape for higher N plasmas as it does for the $N = 2 \times 10^6$ plasma in Fig. 3, this shift should not reduce the cooling rate by more than 10%.

As can be seen in Fig. 4(a), the observed cooling rate Γ is nearly constant out to $N = 1 \times 10^6$, but starts to diminish at higher N . At the highest N we measured, 8×10^7 , the cooling rate is still approximately five times higher than the free

space rate, and approximately ten times higher than the observed off-resonance rate (extrapolated from $N = 5 \times 10^7$). The measured final temperatures [see Fig. 4(b)] begin to climb at approximately $N = 10^5$, and reach the off-resonance value at $N = 8 \times 10^7$.

Numerical studies indicate that the dominant plasma-cavity coupling is through a single center-of-mass cyclotron mode.¹⁵ We believe the rate at which energy is mixed into this mode from the electron ensemble to be the factor limiting cooling for large numbers of electrons, rather than the self-field effect, but further work is needed to determine what causes the mixing at low magnetic field in this cavity.

The cooling effects discussed above were all obtained with plasmas placed at the cavity and mode center. Motivated by our prior work finding that cavity cooling is sometimes the best with plasmas offset from the mode center,⁵ we also studied plasmas placed where the calculated mode amplitude was reduced by a factor of two. In the present cavity, however, we found that offset-plasma cavity cooling is not as efficacious as centered-plasma cavity cooling (see Fig. 4). This remains true at higher magnetic fields and at the corresponding higher order cavity modes, and might be explained by the lower predicted single-particle cooling rate associated with this cavity on account of its greater volume.

The behavior of the final temperatures in Fig. 4 is in rough accord with the predictions of Eq. (1). The cooling rate required to evaluate this formula is directly available from Fig. 4(a). The required heating power H comes, at least in part, from the plasma self-expansion (see Fig. 5). In the presence of collisions, the tendency of like-sign plasma

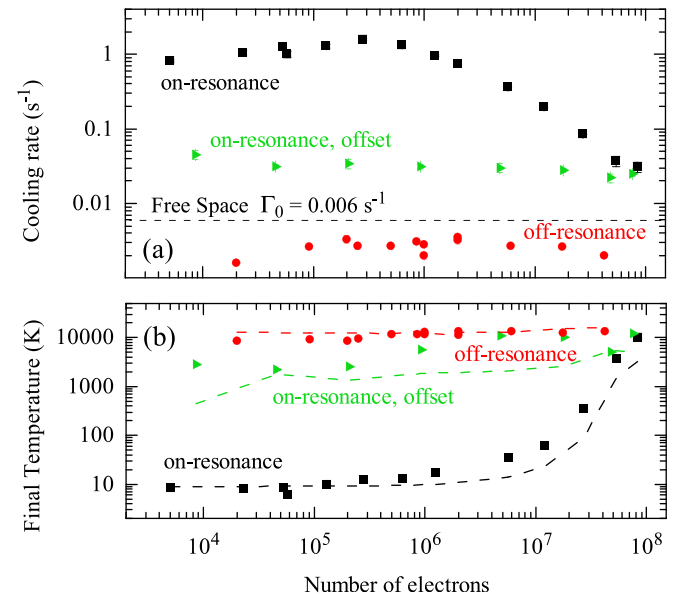


FIG. 4. (a) Cooling rate Γ and (b) final temperature T_F as a function of N . The black square data points were taken with the plasma in the center of the cavity and the field tuned to resonance for 2×10^6 electrons. For green triangular data points, the plasma was held at a 9 cm axial offset from the cavity center, where the microwave field is predicted to be a factor of two weaker. For the red circular data points, the plasma was at the cavity center, but with the field detuned 3 mT away from the cyclotron-cavity resonance. The dashed lines are (a) the free space cooling rate at 0.1555 T and (b) the predicted temperatures at 100 s, including the effect of expansion heating.

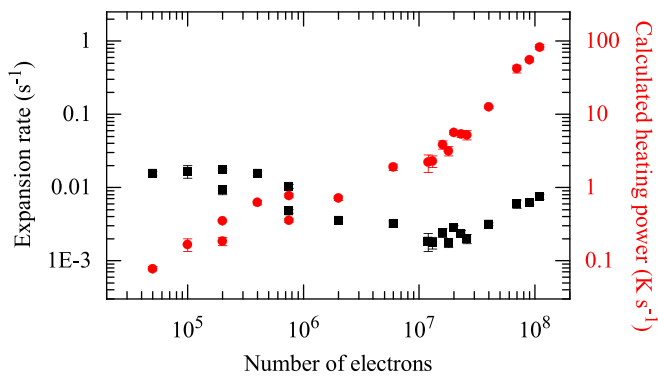


FIG. 5. Measured expansion rate (left axis, black squares) over 100 s and calculated heating power H (right axis, red dots) as a function of N .

particles to separate causes the irreversible conversion of electrostatic potential energy into kinetic energy and ultimately heat.¹⁶ The heating power can be calculated from a formula in Ref. 17, and the result is also plotted in Fig. 5. Using the calculated H , Γ and initial temperature T_0 from the data, along with $T_B = 9$ K, the measured wall temperature, we plot as dashed lines in Fig. 4(b) the predicted temperatures $T_{100s} = T_B + H/\Gamma + (T_0 - T_B - H/\Gamma) \exp[-\Gamma \cdot 100s]$. The prediction agrees with the measured final temperatures at lower N , but slightly underestimates the temperature at higher N for the resonant data set and in general for the offset data set. We suspect that this is an indication of the plasma's increased sensitivity to other heating sources such as electrode voltage noise when it contains more electrons (resonant, high N) or overlaps with multiple electrodes (offset).

V. CONCLUSION

This paper reports a significantly improved range of cooling enhancements compared to our earlier work.⁵ The reason that we observe enhanced cooling for higher numbers of electrons than in Ref. 5 has not yet been definitively established but is believed to involve the rate at which thermal energy is mixed into the dominant radiating mode of the plasma, relative to the single particle cooling rate. The longer, wider cavity structure used here affects both rates via the microwave mode geometry (Γ depends on Q and the effective volume of the mode) and plasma geometry (which influences mixing from bounce motion). Lower temperatures at high N may be the result of improved shielding on the electrode voltage lines or improved alignment of the electric and magnetic fields.

We achieve efficient cavity-enhanced cyclotron cooling at very low magnetic fields: fields low enough that cyclotron cooling is effectively absent without a cavity. The success of this method for $>10^6$ electrons at 0.1555 T suggests that, if expansion heating can be controlled, cooling at even lower field values should be possible. Steady state fields in the 0.15 T range could be provided by a non-superconducting solenoid, which may be preferable for experiments where

precision limits are set by superconducting hysteresis effects,¹⁸ or simply for reduced startup and operating expenses.

Cavity-resonant cooling may also be of interest for some recently proposed experiments involving large numbers of cryogenic leptons in strong magnetic mirror fields,^{19,20} and for antimatter beam experiments which may run at similar magnetic field values. For example, a recent annihilation experiment²¹ was performed using positrons cooled at 0.065 T via sympathetic cooling on a CO buffer gas. Consequently, the final positron temperatures were not lower than the buffer gas temperature, which was held at 50 K to avoid condensation. Our method could potentially remove the need for a buffer gas and also result in greatly reduced energy spread for the beams produced in such an experiment.

ACKNOWLEDGMENTS

We thank F. Robicheaux and T. M. O'Neil for stimulating discussions regarding plasma heating and cooling mechanisms. This work was supported by the DOE DE-FG02-06ER54904, the NSF 1500538-PHY, and the NSERC.

- ¹J. H. Malmberg and J. S. deGrassie, *Phys. Rev. Lett.* **35**, 577 (1975).
- ²R. C. Davidson, *Physics of Nonneutral Plasmas* (Imperial College Press London, 2001), ISBN 978-1860943034.
- ³*Trapped Charged Particles—A Graduate Textbook with Problems and Solutions*, edited by M. Knoop, N. Madsen, and R. C. Thompson (World Scientific Publishing Europe Limited, 2016).
- ⁴T. R. Weber, J. R. Danielson, and C. M. Surko, *Phys. Plasmas* **17**, 123507 (2010).
- ⁵A. P. Povilus, N. D. DeTal, L. T. Evans, N. Evetts, J. Fajans, W. N. Hardy, E. D. Hunter, I. Martens, F. Robicheaux, S. Shanman *et al.*, *Phys. Rev. Lett.* **117**, 175001 (2016).
- ⁶E. M. Purcell, in *Proceedings of the American Physical Society* (American Physical Society, 1946), Vol. 69, p. 681.
- ⁷T. M. O'Neil, *Phys. Fluids* **23**, 725 (1980).
- ⁸G. Gabrielse and H. Dehmelt, *Phys. Rev. Lett.* **55**, 67 (1985).
- ⁹J. Tan and G. Gabrielse, *Phys. Rev. A* **48**, 3105 (1993).
- ¹⁰A. J. Peurrung and J. Fajans, *Rev. Sci. Instrum.* **64**, 52 (1993).
- ¹¹D. L. Eggleston, C. F. Driscoll, B. R. Beck, A. W. Hyatt, and J. H. Malmberg, *Phys. Fluids B* **4**, 3432 (1992).
- ¹²D. Montgomery, G. Joyce, and L. Turner, *Phys. Fluids* **17**, 2201 (1974).
- ¹³N. Evetts, I. Martens, D. Bizzotto, D. Longuevergne, and W. N. Hardy, *Rev. Sci. Instrum.* **87**, 104702 (2016).
- ¹⁴M. Affolter, F. Anderegg, D. H. E. Dubin, and C. F. Driscoll, *Phys. Lett. A* **378**, 2406 (2014).
- ¹⁵F. Robicheaux, personal communication (2017).
- ¹⁶B. P. Cluggish and C. F. Driscoll, *Phys. Rev. Lett.* **74**, 4213 (1995).
- ¹⁷J. R. Danielson, D. H. E. Dubin, R. G. Greaves, and C. M. Surko, *Rev. Mod. Phys.* **87**, 247 (2015).
- ¹⁸C. So, P. Amadruz, W. Bertsche, A. Capra, N. Evetts, J. Fajans, W. Frazer, M. C. Fujiwara, D. Gill, J. Hangst *et al.*, in *APS Division of Nuclear Physics Meeting Abstracts* (Vancouver, 2016).
- ¹⁹R. Gopalan, Ph.D. thesis (University of California, Berkeley, 1998).
- ²⁰R. Lane and C. Ordonez, *J. Phys. B: At. Mol. Opt. Phys.* **49**, 074008 (2016).
- ²¹M. R. Natsin, J. R. Danielson, G. F. Gribakin, A. R. Swann, and C. M. Surko, *Phys. Rev. Lett.* **119**, 113402 (2017).